



# An Improved Preamble Detection Method for LTE-A PRACH Based on Doppler Frequency Offset Correction

Yajing Zhang<sup>1(✉)</sup>, Zhizhong Zhang<sup>2</sup>, and Xiaoling Hu<sup>1,2</sup>

<sup>1</sup> Chongqing University of Posts and Telecommunications, Chongqing, China  
zhangyajing2969@163.com

<sup>2</sup> Test Engineering Research Center of Communication Networks, Chongqing, China

**Abstract.** In the random access process of the Long Term Evolution Advanced (LTE-A) system, the Doppler shift influences the detection of the Physical Random Access Channel (PRACH) signal, resulting in the appearance of the pseudo correlation peaks at the receiving end. In the 3GPP protocol, the frequency offset in the mid-speed and low-speed modes is not processed, and the frequency offset processing algorithm in the high-speed mode only applies to the case where the Doppler frequency offset does not exceed the unit sub-carrier. For solve the problem, a three-step improvement method is proposed. The first step is to perform the maximum likelihood (ML) offset estimation to do the frequency offset correction; the second step is to perform the sliding average filter processing to eliminate the influence of multipath; the third step is to use multiple sliding window peak detection algorithm. Compared with the traditional algorithm, the performance of the proposed method is better. And the false alarm performance under the AWGN channel is at least 3.8 dB better, and the false alarm performance under ETU channel is at least 1 dB better.

**Keywords:** Preamble detection · Frequency offset correction · Sliding average filter processing · Multiple sliding window

## 1 Introduction

The performance evaluation of random access in the Long Term Evolution Advanced (LTE-A) system has become an important research topic in recent years, because the quality of random access will play an important role in the future 5G [1]. The most prominent feature of 5G technology is unmatched speed, which requires shorter access delay and higher random access success rate. The

This work is supported by the National Science and Technology Major Project of the Ministry of Science and Technology of China (2015ZX03001013), the Generic Technology Innovation Project of Key Industries in Chongqing (cstc2017zdcy-zdzz0030), the Innovation Team of University in Chongqing (KJTD201312).

first and most important step in the uplink random access process of the LTE-A system is the successful transmission and correct resolution of the Physical Random Access Channel (PRACH) preamble signal [2]. At the receiving end, the preamble ID and the timing advance (TA) [3] can be correctly parsed by the preamble detection.

The sub-carrier spacing of the random access channel of the LTE-A system is very narrow, It is more susceptible to the influence of frequency offset. In the 3GPP protocol, the frequency offset in the mid-speed and low-speed modes is not processed, and the frequency offset processing algorithm in the high-speed mode only applies to the case where the Doppler frequency offset does not exceed the unit sub-carrier. Therefore, to ensure correct analysis of the random access detection signal, Doppler shift estimation and compensation need to be performed on the uplink.

With regard to the PRACH signal detection technology, experts and scholars at home and abroad have done a lot of research. For example, the preamble detection algorithm for large transmission delay proposed in [4], based on the strong correlation of sequences as an enhanced version of the algorithm to overcome the propagation delay; The ZC sequence grouping and in-group peak sliding detection algorithm proposed in [5], which has efficient hardware implementation by Discrete Fourier Transform (DFT) and large-point Fast Fourier Transform (FFT) algorithm. This type of algorithms do not analyze the increasingly serious effects of frequency offset. Other existing documents do not discuss the effect of preamble detection after frequency offset correction. For example, [6] only studied the frequency offset estimation method of PRACH signal.

Compared with the traditional frequency correlation detection method, this paper mainly completes the detection of the preamble ID signal of random access through Doppler frequency offset correction, sliding average filter processing, multiple sliding window peak detection. And the performance of the proposed method is better.

The remainder of this article is organized as follows. The PRACH signal detection process and effect of Doppler frequency offset on random access signal detection are detailed in Sect. 2. The improved detection method is detailed in Sect. 3. Performance evaluation results that demonstrate the efficiency of the traditional and proposed algorithms are presented in Sect. 4. Conclusions are drawn in Sect. 5.

## 2 Signal Detection and Effect of Frequency Offset

### 2.1 PRACH Signal Detection Process

The random access preamble sequence is generated by the cyclic shift of the Zadoff–Chu (ZC) sequence [2]. Since the ZC sequence just satisfies the good correlation characteristics required for the random access preamble sequence, the definition of ZC sequence is

$$x_u(n) = e^{-j\frac{\pi un(n+1)}{N_{zc}}}, 0 \leq n \leq N_{zc} - 1 \quad (1)$$

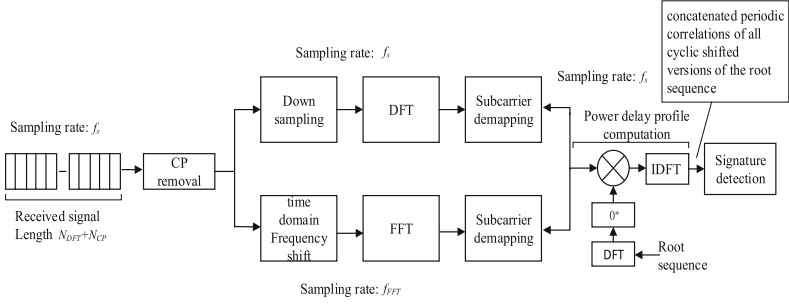


Fig. 1. Random access to the receiving process.

Where  $N_{zc}$  is the length of the ZC sequence,  $u$  is physical root sequence.

The random access preambles with zero correlation zones based on the  $u^{th}$  root ZC sequence with length of  $N_{cs} - 1$  are defined by cyclic shift according to

$$x_{u,v}(n) = x_u((n + C_v) \bmod N_{zc}) \tag{2}$$

Where  $C_v$  is the cyclic shift value and  $N_{cs}$  is the length of cyclic shift.

The random access process eNodeB receiving end [7] is shown in Fig. 1. The preamble signal is synchronized with the local ZC root sequence after CP synchronization, (Cyclic Prefix) CP removal, down sampling, DFT, and sub-carrier selection to obtain correlation values in the frequency domain correlation. And then Inverse Discrete Fourier Transform (IDFT) and modular-squares are performed on correlation values to obtain time-domain correlation energy power delay profile (PDP) sequences. The correlation peak value of PDP sequence is searched by the detection threshold, to judge whether there is random access. If there is random access, preamble ID and timing advance (TA) are calculated.

### 2.2 Effect of Doppler Frequency Offset

When the user equipment (UE) moves fast, a large Doppler shift occurs, affecting the zero auto-correlation of the preamble sequence. Assuming  $\Delta f$  is the Doppler shift, and the define of preamble sequence with containing frequency offset is

$$\begin{aligned} x_u(n, \Delta f) &= e^{-j\frac{\pi u n(n+1)}{N_{zc}}} \cdot e^{j2\pi n \frac{\Delta f}{f_s}} \\ &= x_u(n - d_u) \cdot e^{j2\pi n \frac{\Delta f \cdot T_{seq} - k}{f_s}} \cdot e^{j\phi} \end{aligned} \tag{3}$$

Where  $T_{seq}$  is the last time of preamble sequence,  $f_s$  is the sampling frequency,  $e^{j\phi}$  is a phase rotation constant with modulus 1 and n independent. According to formula 3, preamble sequence has changed with containing Doppler shift. Assuming  $\Delta f = kf_{RA} = k\frac{1}{T_{seq}}$ , the value of displacement is  $d_u$ ,  $d_u$  satisfies  $(d_u \cdot u) \bmod N_{zc} = 1$ , the original main peak completely disappears and the position transfers to  $C_v \pm (k + 1)d_u$ .

Thus, In order to achieve the uplink synchronization between the user equipment and the base station, it is necessary to eliminate the frequency offset on the signal detection at the receiving end.

### 3 Improved Detection Process

#### 3.1 Frequency Offset Estimation and Correction

To analyze the influence of frequency offset, it is necessary to perform frequency offset correction on the receiver signal. In the 3GPP protocol, the frequency offset in the mid-speed and low-speed modes is not processed, and cyclic shift limit set algorithm is used by default in high-speed mode. But frequency offsets in mid-speed and low-speed modes sometimes lead to severe false alarm rates. The cyclic shift limit set algorithm in high-speed mode is computationally complex [8], takes a long time, requires cooperation from the upper layer, and only applies to the case where the Doppler frequency offset does not exceed the unit sub-carrier. Therefore, without considering the UE moving speed, it is better to use the frequency offset estimation method to correct the frequency offset.

The CP in the preamble signal is copied from the last part of the useful signal, and the length of CP is known. According this redundant information, the maximum likelihood (ML) frequency offset estimation method is used to estimate the time and frequency offsets. The signal received from the PRACH channel is modeled from both time and frequency domain, to analyze the time and frequency shift of the signal at the receiving end.

First, the received signal is modeled. The received signal contains the time offset and frequency offset. The time shift is represented by the channel impulse response  $h(n - d)$ . The frequency shift is expressed by multiplying a rotation factor. Thus, the definite of the received signal is

$$r(n) = x(n - d) \cdot e^{j \cdot \frac{2\pi n \Delta f}{N_{zc}}} + w(n) \tag{4}$$

Assuming  $L$  is the length of CP,  $T_{GP}$  is ignored, so the length of the received signal is  $N_{zc} + L$ . Assuming that the time offset and frequency offset are determined, then the probability density function of the  $2N_{zc} + L$  sampling point for the log likelihood function is

$$\wedge (d, \Delta f) = \log f(r(n)|d, \Delta f) \tag{5}$$

Through collection selection and related calculations, all constants and factors that have no effect on the results of the maximum likelihood function are eliminated as useless factors. So the Eq. 5 is simplified to

$$\wedge (d, \Delta f) = \gamma(d) \cos(2\pi \Delta f + \angle \gamma(d)) - \beta \phi(d) \tag{6}$$

where

$$\begin{aligned} \gamma(d) &= \sum_{n-d}^{n-d+L-1} r(n)r^*(n+N) \\ \phi(d) &= \frac{1}{2} \sum_{n-d}^{n-d+L-1} (|r(n)|^2 + |r(n+N)|^2) \\ \beta &= \frac{SNR}{SNR+1} \end{aligned} \tag{7}$$

Equations 6 and 7 indicate that the unknown parameters are  $d$  and  $\Delta f$ . The likelihood function gets the maximum score in two steps. First, let  $d$  be a constant and find the maximum value of the likelihood function corresponding to  $\Delta f$ . When the case is  $\cos(2\pi\Delta f + \angle\gamma(d)) = 1$ , we obtain the maximum value.

$$\begin{aligned} 2\pi\Delta f + \angle\gamma(d) &= 2k\pi \\ \Delta\hat{f}_{ML}(d) &= -\frac{1}{2\pi}\angle\gamma(d) + k \end{aligned} \quad (8)$$

When the frequency offset does not exceed the unit sub-carrier, then  $k = 0$ , and when the frequency offset exceeds the unit sub-carrier, then  $k$  value needs to be calculated by trial. Second, the likelihood function is  $\wedge(d, \Delta\hat{f}_{ML}) = |\gamma(d)| - |\beta\phi(d)|$ . When the likelihood function gets maximum value,  $d$  is estimated. Finally, the  $d$  and  $\Delta f$  are

$$\begin{aligned} \hat{d}_{ML} &= \arg \max_d \{|\angle\gamma(d)| - |\beta\phi(d)|\} \\ \Delta\hat{f}_{ML}(d) &= -\frac{1}{2\pi}\angle\gamma(d) + k \end{aligned} \quad (9)$$

Doppler frequency offset is corrected based on frequency offset value by multiplying frequency deviation factor  $\exp(\frac{j2\pi n\Delta\hat{f}_{ML}}{N_{zc}})$ . TA is calculated by time deviation factor, but base station signal processing complexity is increased and will not be discussed here.

### 3.2 Sliding Average Filter Processing

The sliding average filter is a Finite Impulse Response (FIR) filter with a coefficient of 1. The peak value in the window is processed by the sliding average filter to eliminate the effect of multipath, enhance the intensity of the main peak, and reduce the false alarm probability.

The frequency offset-corrected received signal is multiplied by the local ZC root sequence in the frequency domain, and the result of the time domain correlation is obtained by the IFFT. Then the time domain results of the multiple antennas at the receiving end are summed to obtain the energy-combined PDP spectrum sequence  $p(k)$ .

According to the cyclic shift value and the number of multipaths in different channel models, the value of the *MA\_value* is set,  $MA\_value = MA\_order(k)$ , where  $k = zeroCorrelationZoneConfig + 1$ , values of *zeroCorrelationZoneConfig* and *MA\_order* are listed in Table 1. The value of moving average group delay is calculated by formula  $\lfloor MA\_value/2 \rfloor$ , and the  $N_{shift\_num}$  values at the end of  $p(k)$  are advanced, the end of  $p(k)$  is filled with 0 and the number of 0 is the value of moving average group delay. When the format of preamble is 0 3, the value of  $N_{shift\_num}$  is 3; when the format of preamble is 4, the value of  $N_{shift\_num}$  is 0.

FIR filtering is performed according to the value of *MA\_value*, and then the data of the group delay of  $p(k)$  is removed. a new energy-combined PDP spectrum sequence  $p'(k)$  is obtained, since time domain peak values are corrected by value of *cal\_value*, the value of *cal\_value* is listed in Table 1.

**Table 1.** Different format parameters configuration.

Format 0–3 parameters configuration			
zeroCorrelationZoneConfig	$N_{cs}$	MA_order	cal_value
0	0	7	3
1	13	7	3
2	15	7	3
3	18	7	3
4	22	7	3
...	...	...	...
Format 4 parameters configuration			
zeroCorrelationZoneConfig	$N_{cs}$	MA_order	cal_value
0	2	1	1
1	4	1	1
2	6	3	1
3	8	5	1
4	10	5	1
5	12	5	2

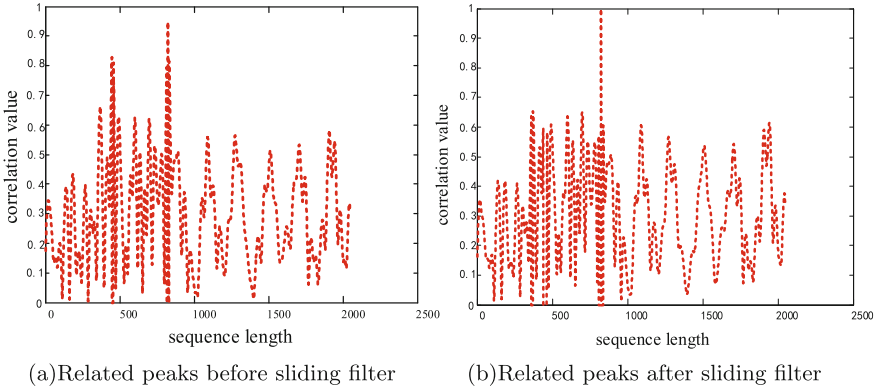


**Fig. 2.** Related peaks change with sliding average filtering.

When the relevant signal output performance deteriorates, the peak energy is not obvious due to noise, and it is not easy to do peak detection. Figure 2 manifest that it is improved by sliding average filter processing to eliminate the effect of multipath, enhance the main peak intensity, and increase the probability of successful detection.

### 3.3 Multiple Sliding Window Peak Detection

On the basis of time-domain peak correction and main peak enhancement, multiple sliding window peak detection is performed, which can further reduce the false alarm rate and increase the success rate of random access.

The noise power is calculated according to the new energy-combined PDP spectrum sequence  $p'(k)$ , and then according to the noise power and protocol requirements that the false alarm rate should be less than 0.1%, the absolute threshold  $Thre\_A$  and the detection threshold  $Thre\_B$  are calculated.

The detection window is divided. According to the new energy-combined PDP spectrum sequence  $p'(k)$ , the detection window is divided by formula 10, and finally divided into 64 detection windows.

$$\begin{cases} main\_win = (2048 * mDetect) / 839 \\ mDetect = 839 - C_v \\ win\_length = 2048 * N_{cs} / 839 \end{cases} \quad (10)$$

Where  $main\_win$  is the position of main window,  $win\_length$  is the length of detection window. Taking format 0 as an example, the preamble sequence length  $N_{zc}$  is 839, and the cyclic shift value  $N_{cs}$  is 13, so a root sequence can generate  $\lfloor 839/13 \rfloor = 64$  preamble sequences, the  $win\_length$  is 31.

Searching for the maximum value of the main detection window through three kinds of rectangular windows with a multiple relationship, the peak value and the position are detected. Using the first sliding rectangular window of length  $N_{cs}$  to slide within each main detection window ( $N_{cs}$  is the minimum non-zero value of the limit set, 13 at low speed, and 15 at high speed), calculate the total energy of the data within the window, search for the peak  $MaxValue\_win1$  of the window and the corresponding starting position; using the second sliding rectangular window of length  $\lfloor \frac{N_{cs}}{2} \rfloor$  to slide within the first sliding rectangular window where the peak is detected, search for the peak  $MaxValue\_win2$  of the window and the corresponding starting position; using the third sliding rectangular window of length  $\lfloor \frac{N_{cs}}{4} \rfloor$  to slide within the second sliding rectangular window where the peak is detected, search for the peak  $MaxValue\_win3$  of the window and the corresponding starting position.

Finally, preamble ID and timing advance are calculated according to the value  $MaxValue\_win3$  and the corresponding starting position.

## 4 Simulation Results

The performance of the preamble detection in LTE-A system is measured by false alarm probability and successful detection probability [9]. According to the protocol requirements of [10], the false alarm probability shall be less than or equal to 0.1%. The probability of successful detection shall be equal to or exceed 99%. According to the noise power and false alarm probability protocol requirements, the random access preamble detection thresholds are obtained by a large number of simulations. The PRACH parameters used in simulation are listed in Table 2.

Figure 3 shows that when the frequency offset is 600 HZ, the proposed method performance is better than traditional method whether it is AWGN channel or ETU channel. Due to the influence of frequency offset, the false alarm rate rises and the detection performance decrease. In this case, the detection threshold needs to be raised. But the proposed method does not need to increase the detection threshold. Under the condition of the false alarm probability is equal to 0.1%, the SNR of the proposed method is about 20 dB when the channel condition is AWGN and the SNR of the proposed method is about 17.8 dB when the channel condition is ETU.

**Table 2.** Simulation parameters.

System bandwidth (MHz)	20
PRACH bandwidth (MHz)	1.08
Sample frequency (MHz)	30.72
FFT point	2048
$N_{zc}$	839
$N_{cs\_index}$	4
Preamble format	0
Subcarrier spacing	1.25
Channel models	AWGN/ETU

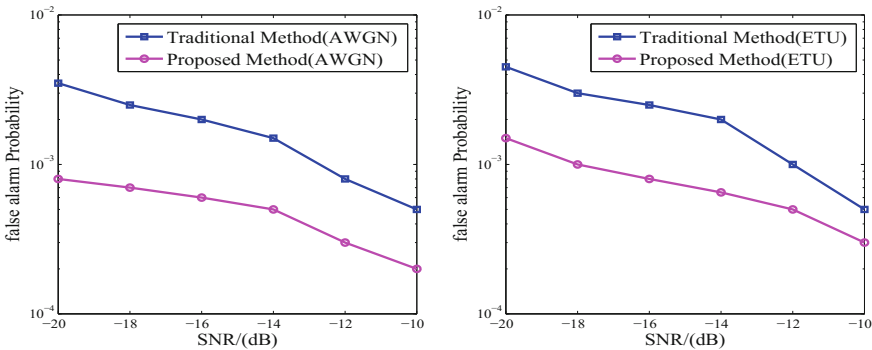


**Fig. 3.** Performance of different methods for 600 Hz frequency offset.

Figure 4 shows that the false alarm probability gradually decreases as the SNR increases. With the increase of SNR in AWGN channel, the reduction of false alarm rate of traditional detection algorithm becomes more and more slowly. However, with the increase of SNR, the reduction of false alarm rate of proposed detection algorithm becomes more increase. The false alarm probability performance is 3.8 dB better than the protocol requirement in AWGN channel and the



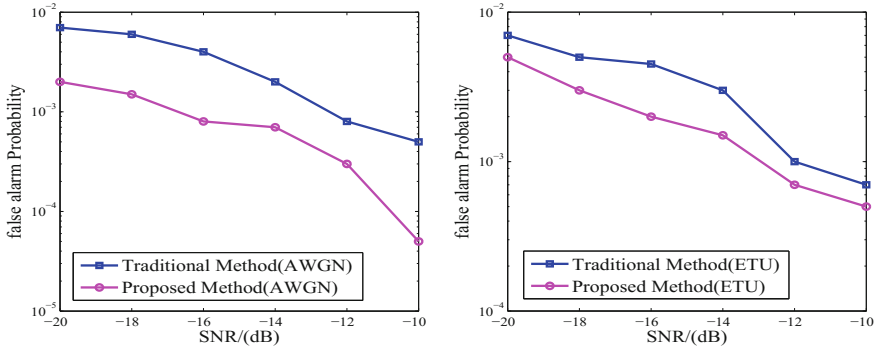


Fig. 4. Performance of different methods for 900 Hz frequency offset.

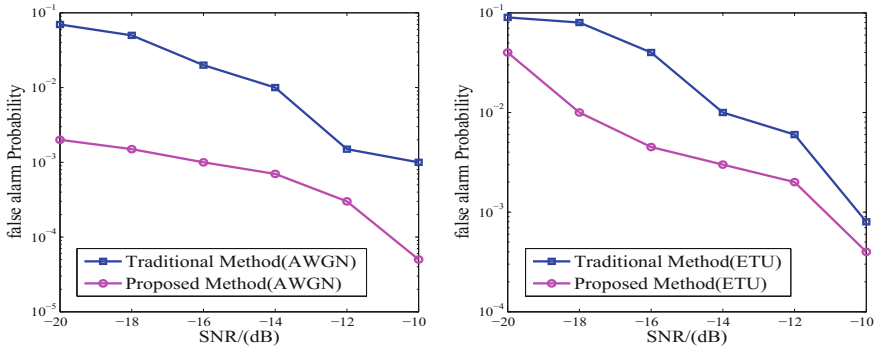


Fig. 5. Performance of different methods for 1500 Hz frequency offset.

false alarm probability performance is 1 dB better than the protocol requirement in ETU channel.

Figure 5 shows the false alarm probability is very large when the frequency offset exceeds 1250 Hz unit sub-carrier. Under the condition of the false alarm probability is equal to 0.1%, the SNR of the proposed method is about 14.7 dB and the SNR of the traditional method is about 10 dB when the channel condition is AWGN. The false alarm probability performance is 1.2 dB better than the traditional method in ETU channel.

In a word, the proposed method has different degrees of performance improvement for different frequency offset. We can draw a conclusion that the false alarm performance under the AWGN channel is at least 3.8 dB better, and the false alarm performance under ETU channel is at least 1 dB better.

## 5 Conclusion

In this paper, we formulated and studied a mixed-combinatorial programming problem for EE optimization in a downlink multiuser OFDM DASs. We divided the optimization problem into two sub-problems, which are DAU selection, and subcarrier assignment and power allocation optimization. Firstly, an energy efficient resource allocation scheme is presented. Then, we transform the optimization problem into a subtractive form, and solved by Lagrangian dual decomposition. From simulation results, we can see the better performance of the proposed algorithm. In the future, the inter-cell interference and cell-edge users' performance will be taken into consideration to how to design EE optimization scheme.

## References

1. 3GPP TS 36.211 V12.3.0 Evolved Universal Terrestrial Radio Access (E-UTRA), Physical channels and modulation, pp. 46–55 (2014)
2. de Figueiredo, F.A.P., Mathilde, F.S., Cardoso, F.A.C.M., Vilela, R.M., Miranda, J.P.: Efficient frequency domain Zadoff-Chu generator with application to LTE and LTE-A systems. In: 2014 International Telecommunications Symposium (ITS), pp. 1–5 (2014)
3. Yang, F., He, Z., Wang, X., Huang, J.: GPP-based random access preamble detection in TD-LTE. In: IEEE Communications and Networking in China (CHINA-COM), pp. 802–806 (2012)
4. Kim, S., Joo, K., Lim, Y.: A delay-robust random access preamble detection algorithm for LTE system. In: IEEE Radio and Wireless Symposium (RWS), pp. 75–78 (2012)
5. Hu, X., Yihui, L., Xiaogang, L.: Research and implementation of PRACH signal detection in LTE-A system. *Appl. Electron. Technol.* **42**(6), 74–76 (2016)
6. Cao, A., Xiao, P., Tafazolli, R.: Frequency offset estimation based on PRACH preambles in LTE. In: IEEE Wireless Communications Systems (ISWCS), pp. 22–26 (2014)
7. Hao, S.: Research on LTE random access detection technology. Xidian University, pp. 50–76 (2015)
8. Li, T., Wang, W., Peng, T.: An improved preamble detection method for LTE PRACH in high-speed railway scenario. In: 2015 10th International Conference on Communications and Networking in China (ChinaCom), Shanghai, pp. 544–549 (2015)
9. Leyva-Mayorga, I., Tello-Oquendo, L., Pla, V., Martinez-Bauset, J., Casares-Giner, V.: On the accurate performance evaluation of the LTE-A random access procedure and the access class barring scheme. In: IEEE Transactions on Wireless Communications, pp. 7785–7799 (2017)
10. Wang, Q., Ren, G., Wu, J.: A multiuser detection algorithm for random access procedure with the presence of carrier frequency offsets in LTE systems. In: IEEE Transactions on Communications, pp. 3299–3312 (2015)